

**Structural Evolution of the  $[(\text{CO}_2)_n(\text{H}_2\text{O})]^-$  Cluster Anions:  
Quantifying the Effect of Hydration on the Excess Charge  
Accommodation Motif**

Journal:	<i>The Journal of Physical Chemistry</i>
Manuscript ID:	jp-2009-03578e
Manuscript Type:	Article
Date Submitted by the Author:	19-Apr-2009
Complete List of Authors:	Nagata, Takashi; The University of Tokyo, Department of Basic Science, Graduate School of Arts & Sciences Muraoka, Azusa; The University of Tokyo, Department of Basic Science, Graduate School of Arts & Sciences Inokuchi, Yoshiya; Hiroshima University, Department of Chemistry, Graduate School of Science Hammer, Nathan; The University of Mississippi, Department of Chemistry & Biochemistry Shin, Joong-Won; Colorado State University, Chemistry Johnson, Mark; Yale University, Chemistry



1  
2  
3  
4  
5  
6  
7  
8  
9  
10  
11  
12  
13  
14  
15  
16  
17  
18  
19  
20  
21  
22  
23  
24  
25  
26  
27  
28  
29  
30  
31  
32  
33  
34  
35  
36  
37  
38  
39  
40  
41  
42  
43  
44  
45  
46  
47  
48  
49  
50  
51  
52  
53  
54  
55  
56  
57  
58  
59  
60

# Structural Evolution of the $[(\text{CO}_2)_n(\text{H}_2\text{O})]^-$ Cluster Anions: Quantifying the Effect of Hydration on the Excess Charge Accommodation Motif

*Azusa Muraoka,<sup>1</sup> Yoshiya Inokuchi,<sup>1, a)</sup> Nathan I. Hammer,<sup>2, b)</sup> Joong-Won Shin,<sup>2, c)</sup> Mark A. Johnson,<sup>2, \*</sup>  
and Takashi Nagata<sup>1, \*</sup>*

<sup>1</sup> Department of Basic Science, Graduate School of Arts and Sciences, The University of Tokyo,  
Komaba, Meguro-ku, Tokyo 153-8902, Japan

<sup>2</sup> Sterling Chemistry Laboratory, Yale University, P.O. Box 208107, New Haven,  
Connecticut 06520

muraoka@tcl.t.u-tokyo.ac.jp, y-inokuchi@hiroshima-u.ac.jp, nhammer@olemiss.edu,  
joongwon@lamar.colostate.edu, mark.johnson@yale.edu, nagata@cluster.c.u-tokyo.ac.jp

**RECEIVED DATE (to be automatically inserted after your manuscript is accepted if required according to the journal that you are submitting your paper to)**

**TITLE RUNNING HEAD:**  $[(\text{CO}_2)_n(\text{H}_2\text{O})]^-$  Cluster Anions

\* Authors to whom correspondence should be addressed. E-mail: nagata@cluster.c.u-tokyo.ac.jp (T. Nagata), mark.johnson@yale.edu (M. A. Johnson).

<sup>a)</sup> Present address: Department of Chemistry, Graduate School of Science, Hiroshima University, Kagamiyama, Higashi-Hiroshima, Hiroshima 739-8526, Japan.

1  
2  
3 b) Present address: Department of Chemistry & Biochemistry, The University of Mississippi, P.O. Box  
4 1848, University, MS 38677  
5

6 c) Present address: Department of Chemistry, Colorado State University, Fort Collins, CO 80523-1872.  
7  
8  
9  
10  
11  
12  
13  
14  
15  
16  
17  
18  
19  
20  
21  
22  
23  
24  
25  
26  
27  
28  
29  
30  
31  
32  
33  
34  
35  
36  
37  
38  
39  
40  
41  
42  
43  
44  
45  
46  
47  
48  
49  
50  
51  
52  
53  
54  
55  
56  
57  
58  
59  
60

1  
2 **Abstract.** The  $[(\text{CO}_2)_n(\text{H}_2\text{O})]^-$  cluster anions are studied using infrared photodissociation (IPD)  
3 spectroscopy in the 2800 – 3800  $\text{cm}^{-1}$  range. The observed IPD spectra display a drastic change in the  
4 vibrational band features at  $n = 4$ , indicating a sharp discontinuity in the structural evolution of the  
5 monohydrated cluster anions. The  $n = 2$  and 3 spectra are composed of a series of sharp bands around  
6 3600  $\text{cm}^{-1}$ , which are assignable to the stretching vibrations of  $\text{H}_2\text{O}$  bound to  $\text{C}_2\text{O}_4^-$  in a double ionic  
7 hydrogen-bonding (DIHB) configuration, as was previously discussed [*J. Chem. Phys.*, **122**, 094303  
8 (2005)]. In the  $n \geq 4$  spectrum, a pair of intense bands additionally appears at  $\approx 3300 \text{ cm}^{-1}$ . With the aid  
9 of ab initio calculations at the MP2/6-31+G\* level, the 3300  $\text{cm}^{-1}$  bands are assigned to the bending  
10 overtone and the hydrogen-bonded OH vibration of  $\text{H}_2\text{O}$  bound to  $\text{CO}_2^-$  via a single O–H...O linkage.  
11 Thus, the structures of  $[(\text{CO}_2)_n(\text{H}_2\text{O})]^-$  evolve with cluster size such that DIHB to  $\text{C}_2\text{O}_4^-$  is favored in  
12 the smaller clusters with  $n = 2$  and 3 whereas  $\text{CO}_2^-$  is preferentially stabilized via the formation of a  
13 single ionic hydrogen-bonding (SIHB) configuration in the larger clusters with  $n \geq 4$ .  
14  
15  
16  
17  
18  
19  
20  
21  
22  
23  
24  
25  
26  
27  
28  
29  
30  
31

32 **Keywords:** Infrared photodissociation spectroscopy, cluster anions, structural evolution, hydration.  
33  
34  
35  
36  
37  
38  
39  
40  
41  
42  
43  
44  
45  
46  
47  
48  
49  
50  
51  
52  
53  
54  
55  
56  
57  
58  
59  
60

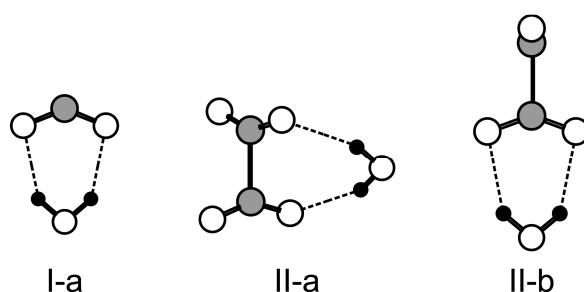
## Introduction

When an excess electron is accommodated by a cluster of molecules, the extent of charge delocalization within the aggregate is primarily governed by the competition between stabilization attained by solvent-induced charge localization and the intrinsic tendency toward charge delocalization through resonance interactions. In the case of carbon dioxide, the charge is either localized on a CO<sub>2</sub> monomer or spread over a dimer moiety to form C<sub>2</sub>O<sub>4</sub><sup>-</sup>, and the resulting (CO<sub>2</sub>)<sub>n</sub><sup>-</sup> cluster anions thus take on an electronic structure represented as either [CO<sub>2</sub><sup>-</sup>·(CO<sub>2</sub>)<sub>n-1</sub>] or [C<sub>2</sub>O<sub>4</sub><sup>-</sup>·(CO<sub>2</sub>)<sub>n-2</sub>].<sup>1-8</sup> These two types of electronic structures, denoted “type I” and “type II”, respectively, can be probed with negative-ion photoelectron spectroscopy by taking advantage of the large difference in vertical detachment energy (VDE) between CO<sub>2</sub><sup>-</sup> and C<sub>2</sub>O<sub>4</sub><sup>-</sup>, which is essentially retained when these core ions are solvated by the remaining CO<sub>2</sub> neutrals.<sup>3, 4, 7</sup> Vibrational spectroscopy provides an even more detailed picture of the core ion structures,<sup>8</sup> where a recent report revealed a dramatically size-dependent “core ion switch,” in which type I clusters dominate in the intermediate size range  $6 \leq n \leq 13$ , while the charge-delocalized, type II forms are predominant at the smaller sizes  $2 \leq n < 6$ . The core ion switching behavior of (CO<sub>2</sub>)<sub>n</sub><sup>-</sup> can be interpreted in the context of the competition between the intrinsic charge delocalization at play in C<sub>2</sub>O<sub>4</sub><sup>-</sup> and the charge localization (onto CO<sub>2</sub><sup>-</sup> monomers) favored when this dimer core ion is exposed to the asymmetrical solvation environments available in the  $n = 6 - 13$  size range.<sup>1, 8</sup>

The “core ion switch” situation changes drastically when a water molecule is incorporated into (CO<sub>2</sub>)<sub>n</sub><sup>-</sup>.<sup>9-13</sup> In Figure 1, photoelectron spectra of [(CO<sub>2</sub>)<sub>n</sub>(H<sub>2</sub>O)]<sup>-</sup> are reproduced along with those of (CO<sub>2</sub>)<sub>n</sub><sup>-</sup> in the size range  $2 \leq n \leq 6$ . The comparison clearly shows the earlier onset of type I clusters upon introduction of one H<sub>2</sub>O molecule into (CO<sub>2</sub>)<sub>n</sub><sup>-</sup>, demonstrating how a solvent molecule capable of hydrogen bonding can dramatically reduce the size required to induce charge localization onto monomeric CO<sub>2</sub><sup>-</sup>. We further explored this effect in an earlier report describing the infrared photodissociation (IPD) spectra of [(CO<sub>2</sub>)<sub>n</sub>(H<sub>2</sub>O)<sub>m</sub>]<sup>-</sup> ( $n = 2, 3$  and  $m = 1, 2$ ) in the 3000 – 3800 cm<sup>-1</sup> region.<sup>13</sup> The spectral patterns were analyzed with the aid of ab initio calculations, leading to the identification of the size- and composition-specific structural motifs by which the incorporated H<sub>2</sub>O

interacts with the core ions. For example, three distinct H-bonding arrangements in the  $[(\text{CO}_2)_{2,3}(\text{H}_2\text{O})]^-$  clusters were identified as depicted in Scheme 1. These motifs, **I-a**, **II-a** and **II-b**, are all derived from the double ionic hydrogen-bonding (DIHB) configuration, where  $\text{H}_2\text{O}$  interacts with the core ion via donation of two equivalent hydrogen bonds. Motif **I-a** is adopted in the type I structure, while **II-a** and **II-b** correspond to the situation at play in the type II species. Considering the spectral changes evident in Figure 1, we now explore how the local interactions evolve at the critical “crossover” cluster  $[(\text{CO}_2)_4(\text{H}_2\text{O})]^-$  where the system displays both type I and type II behavior in same ion packet.

### SCHEME 1



To address this issue, we have extended the IPD spectral measurements of  $[(\text{CO}_2)_n(\text{H}_2\text{O})]^-$  up to  $n = 14$  in the OH stretching region ( $2800 - 3800 \text{ cm}^{-1}$ ). *Ab initio* MO calculations are also carried out to obtain the optimized geometries, vibrational frequencies, and total energies of  $[(\text{CO}_2)_n(\text{H}_2\text{O})]^-$  for the critical size of  $n = 4$ . Combining the experimental observations with the *ab initio* results, we identify the structural motifs appearing in  $[(\text{CO}_2)_n(\text{H}_2\text{O})]^-$  with  $n \geq 4$ , and discuss the origin of the earlier onset for formation of type I structures in the hydrated cluster anions compared to their non-hydrated analogues.

### Experimental

The IPD spectra of  $[(\text{CO}_2)_n(\text{H}_2\text{O})]^-$  ( $n = 2 - 10$  and  $14$ ) were measured in the  $2800\text{--}3800 \text{ cm}^{-1}$  range using the Yale tandem time-of-flight mass spectrometer.<sup>14</sup> The  $[(\text{CO}_2)_n(\text{H}_2\text{O})]^-$  anions were prepared by electron-impact ionization of free jet. A gas mixture of  $\text{CO}_2$  and  $\text{H}_2\text{O}$  was expanded through a pulsed nozzle, and bombarded by a counterpropagating 1-keV electron beam, which produced secondary

1 electrons that were efficiently attached to preexisting  $[(\text{CO}_2)_N(\text{H}_2\text{O})_M]$  neutrals. The cluster anions thus  
2 produced were mass-analyzed by a time-of-flight mass spectrometer, and species with the  $m/e$  of interest  
3 were isolated by a mass gate. The mass-selected anions were then irradiated by an output of a tunable  
4 infrared laser (Nd:YAG-pumped KTP/KTA optical parametric oscillator/amplifier, LaserVision) with an  
5 energy of 5 mJ pulse<sup>-1</sup> and a bandwidth of about 2 cm<sup>-1</sup>. The infrared excitation resulted in the  
6 vibrational predissociation of the cluster anions:  $[(\text{CO}_2)_n(\text{H}_2\text{O})]^- + h\nu \rightarrow [(\text{CO}_2)_{n-1}(\text{H}_2\text{O})]^- + \text{CO}_2$ . The  
7 resultant fragment ions were mass-analyzed by a reflectron and detected by a microchannel ion detector.  
8 The IPD spectra of  $[(\text{CO}_2)_n(\text{H}_2\text{O})]^-$  were obtained by plotting the yields of photofragment ions as a  
9 function of the infrared photon energy.  
10  
11  
12  
13  
14  
15  
16  
17  
18  
19  
20  
21  
22  
23

## 24 Results and Discussion

### 25 A. General features of IPD spectra

26 Figure 2 displays an overview of the IPD spectra of  $[(\text{CO}_2)_n(\text{H}_2\text{O})]^-$  ( $n = 2 - 10$  and 14) measured in  
27 the 2800–3800 cm<sup>-1</sup> range. Although the bands are somewhat better resolved, for  $n = 2$  and 3, the  
28 features in the 3400 – 3800 cm<sup>-1</sup> range are identical to those observed in our previous measurement.<sup>13</sup>  
29 The band positions recorded by the two sets of measurements agree quite well with one another: sharp  
30 bands appear at 3570 and 3618 cm<sup>-1</sup> (3570 and 3618 cm<sup>-1</sup> in the previous study<sup>13</sup>) in the  $n = 2$  spectrum,  
31 and at 3580 and 3620 cm<sup>-1</sup> (vs 3577 and 3620 cm<sup>-1</sup>)<sup>13</sup> in  $n = 3$  along with a weak hump around 3530  
32 cm<sup>-1</sup>. In addition to these higher energy features, the larger spectral range available with the present  
33 laser system revealed a new series of bands in the 3000 – 3200 cm<sup>-1</sup> region (for  $n = 2$ ), and although  
34 weaker, they are still discernable in the  $n = 3$  spectrum. The  $n = 4$  spectrum displays the most complex  
35 array of bands of all clusters studied. The overlapping triplet with peaks at 3530, 3590 and 3620 cm<sup>-1</sup> is  
36 reminiscent of the structure found in the  $n = 2$  and 3 spectra in this energy range, except for the  
37 enhanced intensity of the peak at 3530 cm<sup>-1</sup>. The  $n = 4$  spectrum also exhibits a tiny peak at 2920 cm<sup>-1</sup>,  
38 a sharp peak at 3705 cm<sup>-1</sup>, and a strong, broad doublet with maxima at 3270 and 3370 cm<sup>-1</sup>. The  
39  $[(\text{CO}_2)_n(\text{H}_2\text{O})]^-$  species with  $n \geq 5$  display almost identical IPD spectral profiles; they consist of a sharp  
40  
41  
42  
43  
44  
45  
46  
47  
48  
49  
50  
51  
52  
53  
54  
55  
56  
57  
58  
59  
60

1 peak at  $\approx 3710\text{ cm}^{-1}$ , broad bands at  $\approx 3270$  and  $\approx 3370\text{ cm}^{-1}$ , and tiny peaks at  $\approx 2920$ ,  $\approx 3600$  and  $\approx 3650$   
2  
3  $\text{cm}^{-1}$ . Thus, the IPD spectral features of the  $[(\text{CO}_2)_n(\text{H}_2\text{O})]^-$  species evolve with the cluster size as  
4  
5 follows: (1) the  $n = 2$  and 3 spectra have almost identical band structures around  $3600\text{ cm}^{-1}$ , (2) these  
6  
7 are retained in the  $n = 4$  spectrum, while new features appear around  $3300\text{ cm}^{-1}$  along with peaks at  
8  
9  $2920$  and  $3705\text{ cm}^{-1}$ , (3) the  $\approx 3600\text{ cm}^{-1}$  bands disappear at  $n = 5$ , whereas the  $\approx 3300\text{ cm}^{-1}$  doublet,  
10  
11 along with the  $2920$  and  $3705\text{ cm}^{-1}$  peaks, remain almost intact in the  $n = 5$  spectrum, (4) the spectral  
12  
13 pattern is essential constant for  $n \geq 5$ . From these experimental findings, it can be inferred that the  
14  
15 hydrogen-bonded structures formed in the larger  $[(\text{CO}_2)_n(\text{H}_2\text{O})]^-$  clusters are quite different from those  
16  
17 occurring in their smaller analogues. The structural change begins promptly at  $n = 4$ , where previous  
18  
19 work<sup>10</sup> established the presence of two types of electronic isomers,  $[\text{C}_2\text{O}_4^- \cdot (\text{CO}_2)_{n-2}(\text{H}_2\text{O})]^-$  and  
20  
21  $[\text{CO}_2^- \cdot (\text{CO}_2)_{n-1}(\text{H}_2\text{O})]^-$ , that coexist with comparable populations.  
22  
23  
24  
25

## 26 B. Spectral assignments

### 27 1. $[(\text{CO}_2)_n(\text{H}_2\text{O})]^-$ with $n = 2$ and 3

28  
29  
30  
31 The vibrational assignments for the  $[(\text{CO}_2)_n(\text{H}_2\text{O})]^-$  ( $n = 2$  and 3) spectra in the  $3400 - 3800\text{ cm}^{-1}$   
32  
33 range have been described in detail in Ref. 13. Briefly, the bands are derived from water molecules  
34  
35 binding to the core ion in a DIHB configuration. In this scheme, the  $3570$  and  $3618\text{ cm}^{-1}$  bands in the  $n$   
36  
37  $= 2$  spectrum ( $3580$  and  $3620\text{ cm}^{-1}$  in  $n = 3$ ) are assigned respectively to the symmetric and asymmetric  
38  
39 OH stretching vibrations of the  $\text{H}_2\text{O}$  molecule forming the ring structure with  $\text{C}_2\text{O}_4^-$  (Motif **II-a** or **II-**  
40  
41 **b**). The weaker hump around  $3530\text{ cm}^{-1}$  is less clear, and has been ascribed to the symmetric OH  
42  
43 stretching vibration of the  $\text{H}_2\text{O}$  molecule that participates in the formation of a ring structure with  $\text{CO}_2^-$   
44  
45 (Motif **I-a**). For readers' convenience, Figure 3 reproduces the optimized structures for  $[(\text{CO}_2)_2,$   
46  
47  ${}_3(\text{H}_2\text{O})]^-$  isomers which were identified as the IPD spectral carriers in the previous study.<sup>11, 13</sup>  
48  
49  
50  
51

52 The new series of bands observed in the lower energy  $3000 - 3200\text{ cm}^{-1}$  range closely resemble those  
53  
54 observed in the IPD spectrum of  $(\text{CO}_2)_3^-$ ,<sup>8</sup> and are thus associated with the dimer anion known<sup>10</sup> to be  
55  
56 the core ion in  $[(\text{CO}_2)_{2,3}(\text{H}_2\text{O})]^-$ . Specifically, these are assigned to combination bands involving the  $\nu_5$   
57  
58  
59  
60



1 +  $\nu_7 + x\nu_4$  ( $x = 0$  and 1) modes of  $C_2O_4^-$  which are remarkably unperturbed when the ion is coordinated  
2  
3 directly to a water molecule.

## 4 2. $[(CO_2)_n(H_2O)]^-$ with $n = 4$

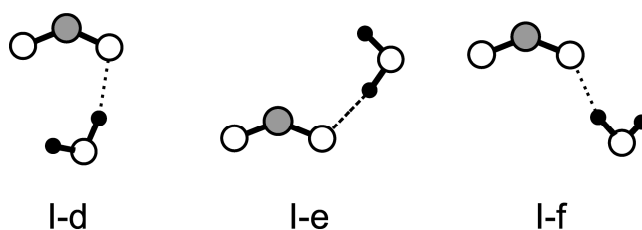
5  
6  
7 Based on the above discussion of the  $n = 2$  and 3 spectra, assignment of the  $[(CO_2)_4(H_2O)]^-$   
8  
9 vibrational bands around  $3600\text{ cm}^{-1}$  is straightforward. The  $3590$  and  $3620\text{ cm}^{-1}$  bands can be traced to  
10  
11 the symmetric and the asymmetric OH stretching vibrations of an  $H_2O$  molecule involved in the ring  
12  
13 structure composed of  $C_2O_4^-$  and  $H_2O$  (**II-a** and **II-b** in Scheme 1), while the  $3530\text{ cm}^{-1}$  band appears in  
14  
15 the location of the symmetric OH stretching vibration of  $H_2O$  bound to a  $CO_2^-$  monomer core in a DIHB  
16  
17 manner (**I-a**). The enhanced relative contribution of the  $3530\text{ cm}^{-1}$  band then suggests an increasing  
18  
19 population of  $[(CO_2)_4(H_2O)]^-$  isomers containing motif **I-a**. Assignment of the  $2920$  and  $3705\text{ cm}^{-1}$   
20  
21 bands is also straightforward based on comparison with IPD spectrum of  $(CO_2)_n^-$ ,<sup>8</sup> where similar  
22  
23 features occur and are identified as the  $\nu_1 + \nu_3$  combination bands of  $CO_2^-$  and  $CO_2$ , respectively. Once  
24  
25 again, the  $\nu_5 + \nu_7 + x\nu_4$  combination bands of  $C_2O_4^-$  are weak but evident in the  $3000 - 3200\text{ cm}^{-1}$   
26  
27 range. These assignments are consistent with the fact that  $CO_2^-(CO_2)_3(H_2O)$  and  $C_2O_4^-(CO_2)_2(H_2O)$   
28  
29 isomeric forms are coexisting in  $[(CO_2)_4(H_2O)]^-$ .  
30  
31  
32  
33  
34  
35

36 The other dominant feature of the  $n = 4$  spectrum is the broad doublet emerging around  $3300\text{ cm}^{-1}$ . A  
37  
38 key to the assignment of this structure is its strong resemblance to the pattern found in  $[(CO_2)_1(H_2O)_2]^-$   
39  
40 ( $3249$  and  $3345$  vs  $3270$  and  $3370\text{ cm}^{-1}$ ) where it was traced<sup>13</sup> to the overtone of the bending and  
41  
42 hydrogen-bonded OH stretching vibrations of the  $H_2O$  molecules, which are independently bound to the  
43  
44 O atoms of  $CO_2^-$ . We can therefore infer that one of the  $[(CO_2)_4(H_2O)]^-$  isomers contains a structural  
45  
46 motif where  $H_2O$  interacts with  $CO_2^-$  only via a single hydrogen bond (SIHB configuration). We next  
47  
48 turn to ab initio calculations to further explore this possibility.  
49  
50  
51

52 Ab initio MO calculations for  $[(CO_2)_4(H_2O)]^-$  were performed by using the GAUSSIAN98 program  
53  
54 package.<sup>15</sup> Geometry optimizations and vibrational analyses were carried out at the MP2/6-31+G\*  
55  
56 level. In order to compare the calculated vibrational transition energies with the observed spectra, a  
57  
58 scaling factor of 0.9696 was employed. This factor was determined so as to reproduce the OH  
59  
60

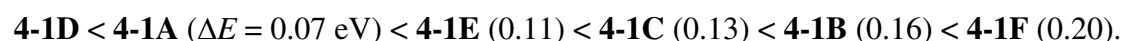
stretching frequencies of an isolated H<sub>2</sub>O molecule. In Figure 4, the observed IPD spectrum is compared with the calculated vibrational patterns along with the optimized geometries for [(CO<sub>2</sub>)<sub>4</sub>(H<sub>2</sub>O)]<sup>-</sup>, which can be classified systematically into six groups according to their structural motifs. The present MP2 calculations actually recovered 24 stable isomeric forms for [(CO<sub>2</sub>)<sub>4</sub>(H<sub>2</sub>O)]<sup>-</sup>, and the optimized structures displayed in Figure 4 correspond to the lowest-energy representatives of each group. Among these six isomeric forms, three (**4-1A** – **4-1C**) possess a DIHB configuration (motifs **I-a**, **II-a** and **II-b**), and species **4-1A** – **4-1C** could account for the higher energy OH stretching bands observed at 3530, 3590 and 3620 cm<sup>-1</sup>. The other three forms (**4-1D** – **4-1F**) have an SIHB configuration, where the H<sub>2</sub>O molecule is hydrogen-bonded to CO<sub>2</sub><sup>-</sup> through a single O–H...O linkage. The calculated vibrational patterns for **4-1D** – **4-1F** exhibit an intense transition in the 3300 – 3400 cm<sup>-1</sup> range, which arises from the hydrogen-bonded OH stretching vibration of H<sub>2</sub>O, thus accounting for the 3370 cm<sup>-1</sup> band. On the analogy of the [(CO<sub>2</sub>)<sub>n</sub>(H<sub>2</sub>O)<sub>2</sub>]<sup>-</sup> (*n* = 1 – 3) case, the 3270 cm<sup>-1</sup> band is ascribed to the overtone of the H<sub>2</sub>O bending vibration,<sup>13</sup> the intensity of which is enhanced via resonance coupling with the 3370 cm<sup>-1</sup> transition. Although the vibrational frequency predicted for the hydrogen-bonded OH stretching vibration in **4-1E** (3271 cm<sup>-1</sup>) is in excellent agreement with the observed frequency (3270 cm<sup>-1</sup>) this could be coincidental given the expected accuracy of the calculations. Theory also predicts a weak band around 3700 cm<sup>-1</sup> for **4-1D** – **4-1F**, which corresponds to the free OH stretching vibration of the hydrogen-bonded H<sub>2</sub>O, but this feature would probably be lost due to overlap with the (*ν*<sub>1</sub> + *ν*<sub>3</sub>) combination band of CO<sub>2</sub> at 3705 cm<sup>-1</sup>. Analysis of the minimum energy structures reveals three anionic H-bonding structural motifs first appearing at *n* = 4, which are denoted **I-d**, **I-e**, and **I-f**, respectively in Scheme 2.

## SCHEME 2



Of course, the assignment of the doublet to a Fermi-resonance interaction can be directly tested by isotopic substitution. Therefore, to reinforce the above argument, we have also examined the IPD spectra of isotopic-substituted species,  $[(\text{CO}_2)_4(\text{HDO})]^-$  and  $[(\text{CO}_2)_4(\text{D}_2\text{O})]^-$ . The resulting spectra are shown in Figure 5, and the twin peaks around  $3300\text{ cm}^{-1}$  indeed collapse into a single broad feature in  $[(\text{CO}_2)_4(\text{HDO})]^-$  before disappearing in  $[(\text{CO}_2)_4(\text{D}_2\text{O})]^-$ . This evolution is easily understood on the basis of the ab initio results also shown in Figure 5, where the stick diagrams of the calculated vibrational frequencies are displayed for the two isotopomers arising from the singly deuterated **4-1D** species. In discussing the results in Figure 5, the essential features are the frequencies of the  $2\nu_2$  bending overtones relative to the H-bonded OH stretches, given a mixing matrix element close to  $35\text{ cm}^{-1}$ .<sup>16</sup> The  $2\nu_2$  transition is calculated to be close enough to interact with the hydrogen-bonded OH stretching vibration in  $(\text{CO}_2)_3\cdot\text{CO}_2^-\cdots\text{H}-\text{OH}$ , while this is not the case in both  $(\text{CO}_2)_3\cdot\text{CO}_2^-\cdots\text{H}-\text{OD}$  and  $(\text{CO}_2)_3\cdot\text{CO}_2^-\cdots\text{D}-\text{OH}$ . These results are thus consistent with assignment of the doublet to resonance coupling between the hydrogen-bonded OH stretching vibration and the  $2\nu_2$  bending overtone in normal  $[(\text{CO}_2)_4(\text{H}_2\text{O})]^-$  species.

The total energies of the  $[(\text{CO}_2)_4(\text{H}_2\text{O})]^-$  local minima were evaluated by carrying out single-point energy calculations at the CCSDT/6-31+G\* level with the optimized structures obtained in the MP2/6-31+G\* calculations (CCSDT/6-31+G\*/MP2/6-31+G\*). Structure **4-1D** is recovered as the global minimum with an energy ordering as follows:



Note that **4-1D** is a type I structure ( $\text{CO}_2^-$  core), in contrast to the  $[(\text{CO}_2)_{2,3}(\text{H}_2\text{O})]^-$  cases, where the most stable isomeric forms, **2-1A** and **3-1A**, both have type II structures with a  $\text{C}_2\text{O}_4^-$  core.

### 3. $[(\text{CO}_2)_n(\text{H}_2\text{O})]^-$ with $n \geq 5$

The IPD spectra for  $n \geq 5$  are simpler than those for  $n < 5$  and are consistent with a scenario where they all occur as type I isomers best represented as  $[\text{CO}_2^-\cdot(\text{CO}_2)_{n-1}(\text{H}_2\text{O})]$  (see Figure 1). We could not

attempt ab initio calculations for these larger species as they are both computationally too demanding and occur with increasingly complex potential surfaces giving rise to large numbers of local minima. However, the persistence of the bands already present in the type I form of the  $n = 4$  cluster, together with the absence of any new features emerging at larger size, these are based on the **I-d**, **I-e** and **I-f** structural subunits, which give rise to the two prominent peaks in the  $3500\text{ cm}^{-1}$  region through the resonant coupling mechanism between the HOH bend overtone and the bound OH stretch fundamental. As in the case of  $n = 4$ , the  $2920$  and  $3705\text{ cm}^{-1}$  bands are assigned to the combination of  $\nu_1 + \nu_3$  of  $\text{CO}_2^-$  and  $\text{CO}_2$ , respectively. A pair of weak bands are now clearly resolved around  $3600\text{ cm}^{-1}$  which are evident because of the absence of the overlapping high energy bands arising from type II structures. These were observed in the previous study of  $(\text{CO}_2)_n^-$ ; the  $3590\text{ cm}^{-1}$  band is due to the  $2\nu_2 + \nu_3$  combination of  $\text{CO}_2$  while the  $3645\text{ cm}^{-1}$  feature is traced to the  $\nu_1 + \nu_2 + \nu_3$  mode of  $\text{CO}_2^-$ .<sup>8</sup> The relative intensities of the  $3590$  and  $3705\text{ cm}^{-1}$  bands tend to increase with cluster size as can be anticipated from the increasing numbers of  $\text{CO}_2$  solvent molecules.

### C. Structural evolution in $[(\text{CO}_2)_n(\text{H}_2\text{O})]^-$

On the bases of the findings described above, we are now in a position to discuss the structural evolution in  $[(\text{CO}_2)_n(\text{H}_2\text{O})]^-$ . First, let us summarize the core ion formation and hydration motifs occurring in  $[(\text{CO}_2)_n(\text{H}_2\text{O})]^-$ . For the  $n = 2$  and 3 species, the dominant isomers take on type II structures ( $\text{C}_2\text{O}_4^-$  cores) containing motifs **II-a** and **II-b**. The type I isomer ( $\text{CO}_2^-$  core) with motif **I-a** is only a minor species at  $n = 2$  and 3. All these structural motifs, **I-a**, **II-a** and **II-b**, belong to the DIHB configuration. At  $n = 4$ , the type I and II isomers have comparable populations.<sup>10</sup> The increase in the type I population introduces new isomeric forms having motifs **I-d** – **I-f**. All these can be characterized as “open” structures with SIHB configurations, where the  $\text{CO}_2^-$  ion core interacts with  $\text{H}_2\text{O}$  through a single  $\text{O-H}\cdots\text{O}$  hydrogen bond. For the larger clusters with  $n \geq 5$ , only type I isomers appear which retain the spectral signatures of the **I-d** – **I-f** motifs. It is important to note that ab initio calculations predict many isomeric forms that exhibit similar local hydration motifs but differ according to their overall geometries. As these have almost identical vibrational patterns, we have highlighted isomeric

1 forms **4-1D** – **4-1F** as representatives of the spectral carriers on the basis that they are recovered as low  
2 energy forms within this class.  
3

4  
5 The present findings raise the naive question of whether we can identify the leading factors that  
6 contribute to the structural evolution in  $[(\text{CO}_2)_n(\text{H}_2\text{O})]^-$ . Generally, ionic systems gain their stabilization  
7 energies by charge delocalization through resonance interactions (when available) and/or by electrostatic  
8 interactions with surrounding solvents. In the smaller  $[(\text{CO}_2)_n(\text{H}_2\text{O})]^-$  clusters such as the  $n = 2$  and 3  
9 species, only a restricted number of molecules are available for solvation and, consequently, the excess  
10 charge tends to be delocalized over two  $\text{CO}_2$  molecules through the charge-resonance interaction,  
11 resulting in a type II structure. As the excess charge is delocalized equally on the terminal O atoms in  
12  $\text{C}_2\text{O}_4^-$ ,<sup>1</sup>  $\text{H}_2\text{O}$  interacts with the  $\text{C}_2\text{O}_4^-$  core as it tends to do with large excess charge distributions, i.e.,  
13 through formation of the DIHB configuration. This inference is supported quantitatively by the ab initio  
14 results which indicate that **2-1A** and **3-1A** (Figure 3) are the global minimum structures for  $n = 2$  and  
15 3.<sup>11, 13</sup> It should be also noted that the separation between the terminal oxygen atoms of the  $\text{C}_2\text{O}_4^-$  core  
16 is calculated to be 2.96 Å in **2-1A** and 3.02 Å in **3-1A**,<sup>17</sup> which provides favorable binding sites for  
17 stable DIHB configurations.<sup>18</sup> Hence, the  $\text{C}_2\text{O}_4^- \cdot \text{H}_2\text{O}$  component assembles predominantly with a DIHB  
18 configuration in  $[(\text{CO}_2)_{2,3}(\text{H}_2\text{O})]^-$ . When the cluster size is increased, the number of solvent molecules  
19 increases and, as a result, stabilization due to solvation begins to make a dominant contribution.  
20 Intuitively, the system gains a larger amount of solvation energy through the electrostatic interactions  
21 when a larger number of neutral molecules occupy the solvation sites around the core ion. As discussed  
22 at length in the context of charge localization in the homogeneous  $(\text{CO}_2)_n^-$  system,<sup>8</sup> asymmetrical  
23 solvation induces charge localization onto a single  $\text{CO}_2^-$  molecule. When this occurs, the distance  
24 between the oxygen atoms is too small to support the DIHB motif, and the monohydrate adopts an SIHB  
25 configuration. The present experimental results indicate that this situation is first achieved at  $n = 4$  with  
26 the **4-1D** configuration, as also revealed by the ab initio energy ordering, and that the situation does not  
27 change in the larger  $[(\text{CO}_2)_n(\text{H}_2\text{O})]^-$  clusters with  $n \geq 5$ .  
28  
29  
30  
31  
32  
33  
34  
35  
36  
37  
38  
39  
40  
41  
42  
43  
44  
45  
46  
47  
48  
49  
50  
51  
52  
53  
54  
55  
56  
57  
58  
59  
60

1 It is interesting to compare the “core ion switch” behavior shown in  $[(\text{CO}_2)_n(\text{H}_2\text{O})]^-$  with those in  
2  $(\text{CO}_2)_n^-$  and  $[(\text{CO}_2)_n(\text{CH}_3\text{OH})]^-$  in terms of the minimum cluster size at which type I becomes  
3 predominant. By counting the total number of constituent molecules, the minimum size is 6 for  
4  $(\text{CO}_2)_n^-$ ,<sup>3</sup> 5 for  $[(\text{CO}_2)_n(\text{H}_2\text{O})]^-$ ,<sup>10</sup> and 3 for  $[(\text{CO}_2)_n(\text{CH}_3\text{OH})]^-$ .<sup>10, 19</sup> According to the previous  
5 discussion on the origin of the core ion switch,<sup>8</sup> the driving force for promoting the  $\text{CO}_2^-$  formation is  
6 traced to the asymmetric solvation environment surrounding the core ion. In the  $(\text{CO}_2)_n^-$  case, solvent  
7 asymmetry arises from the incompleteness of the first solvation shell in the size range  $6 \leq n \leq 13$ . In  
8 contrast, solvation shells intrinsically occur asymmetrically in the heterogeneous  $[(\text{CO}_2)_n(\text{H}_2\text{O})]^-$  and  
9  $[(\text{CO}_2)_n(\text{CH}_3\text{OH})]^-$  clusters. Taking into consideration the fact that type I isomers appear as major  
10 species even at  $n = 2$  in the  $[(\text{CO}_2)_n(\text{CH}_3\text{OH})]^-$  case,<sup>10</sup> we infer that the local aspects of the H-bonding  
11 interaction in  $[(\text{CO}_2)_n(\text{CH}_3\text{OH})]^-$  become a main cause for charge localization. That is, since methanol  
12 can only donate one H-bond, the DIHB arrangement that is preferred for type II clusters is not available.  
13 Seen from this viewpoint, the present  $[(\text{CO}_2)_n(\text{H}_2\text{O})]^-$  results suggest that the ability of  $\text{H}_2\text{O}$  to form a  
14 DIHB configuration allows the type II forms to persist to larger size in the hydrates. It is not until  $n = 4$   
15 that the neutral  $\text{CO}_2$  solvent molecules overpower this intrinsic type II motif and drive the system toward  
16 charge localized clusters with type I cores.

## 40 Conclusion

41  
42 In summary, we report infrared photodissociation (IPD) spectra of  $[(\text{CO}_2)_n(\text{H}_2\text{O})]^-$  ( $n = 2 - 10, 14$ ) in  
43 the  $2800 - 3800 \text{ cm}^{-1}$  range and interpret the results with ab initio calculations. The observed IPD  
44 spectra can be classified into two groups according to their patterns of hydrogen-bonded OH stretching  
45 vibrations. The  $n = 2$  and 3 spectra are characterized by a series of sharp bands around  $3600 \text{ cm}^{-1}$ ,  
46 whereas the  $n > 4$  spectra are dominated exclusively by a broad doublet around  $3300 \text{ cm}^{-1}$  along with  
47 transitions arising from neutral  $\text{CO}_2$  and the  $\text{CO}_2^-$  core ion. Interestingly, both groups of bands appear in  
48 the  $n = 4$  spectrum. This new spectroscopic information confirms the previous conclusions based on  
49 photoelectron spectroscopy<sup>10, 12</sup> that type II isomers ( $\text{C}_2\text{O}_4^-$  core) are preferably formed in  $[(\text{CO}_2)_2,$   
50  
51  
52  
53  
54  
55  
56  
57  
58  
59  
60

1  
2  
3  
4  
5  
6  
7  
8  
9  
10  
11  
12  
13  
14  
15  
16  
17  
18  
19  
20  
21  
22  
23  
24  
25  
26  
27  
28  
29  
30  
31  
32  
33  
34  
35  
36  
37  
38  
39  
40  
41  
42  
43  
44  
45  
46  
47  
48  
49  
50  
51  
52  
53  
54  
55  
56  
57  
58  
59  
60

${}_3(\text{H}_2\text{O})]^-$  while type I isomers ( $\text{CO}_2^-$  core) become dominant in  $[(\text{CO}_2)_n(\text{H}_2\text{O})]^-$  with  $n > 4$ ; both types coexist at  $n = 4$ . The band patterns provide more precise information on the hydrogen-bonding structures at play, where the  $[(\text{CO}_2)_{2,3}(\text{H}_2\text{O})]^-$  clusters occur with both hydrogen atoms of the water molecule engaged in anionic hydrogen bonds, and the larger clusters  $[(\text{CO}_2)_{n>4}(\text{H}_2\text{O})]^-$  occur with the single anionic H-bonding motif. Through the structural evolution shown in  $[(\text{CO}_2)_n(\text{H}_2\text{O})]^-$ ,  $\text{H}_2\text{O}$  demonstrates its ability to bridge across the charge-delocalized  $\text{C}_2\text{O}_4^-$  core ion, acting to reinforce the dimer structure, as well as contribute to the destruction of the dimer by tightly binding to one of the constituents, causing charge localization onto the  $\text{CO}_2^-$  monomer core ion.

**Acknowledgment.** The authors are grateful to Professor K. Takatsuka for the loan of high-performance computers. A part of the ab initio calculations was performed by using the computer systems at Research Center for Computational Science, Okazaki Research Facilities, National Institutes of Natural Sciences (NINS). This work is partly supported by Grants-in-Aid for Scientific Research (Grants 18550007, 19029011 and 20038015) from the Japan Society for the Promotion of Science (JSPS), and from the Ministry of Education, Culture, Sports, Science and Technology (MEXT). MAJ thanks the Department of Energy for support of this work under grant DE-FG02-06ER15800.

**Supporting Information Available:** Structure parameters for the  $[(\text{CO}_2)_4(\text{H}_2\text{O})]^-$  isomeric forms shown in Fig. 4 (MP2/6-31+G\*). The material is available free of charge via the Internet at <http://pubs.acs.org>. The structure parameters for all the  $[(\text{CO}_2)_4(\text{H}_2\text{O})]^-$  isomers obtained in the present study are also available on request.

## References

- 1  
2  
3 (1) Fleischman, S. H.; Jordan, K. D. *J. Phys. Chem.* **1987**, 91, 1300.
- 4  
5  
6 (2) Bowen, K. H.; Eaton, J. G. In *The Structure of Small Molecules and Ions*; Naaman, R., Vagar, Z.,  
7  
8 Eds.; Plenum Press, New York, **1987**; p. 147.
- 9  
10  
11 (3) DeLuca, M. J.; Niu, B.; Johnson, M. A. *J. Chem. Phys.* **1988**, 88, 5857.
- 12  
13  
14 (4) Tsukuda, T.; Johnson, M. A.; Nagata, T. *Chem. Phys. Lett.* **1997**, 268, 429.
- 15  
16  
17 (5) Saeki, M.; Tsukuda, T.; Nagata, T. *Chem. Phys. Lett.* **2001**, 340, 376.
- 18  
19  
20 (6) Sommerfeld, T.; Posset, T. *J. Chem. Phys.* **2003**, 119, 7714.
- 21  
22  
23 (7) Mabbs, R.; Surber, E.; Velarde, L.; Sanov, A. *J. Chem. Phys.* **2004**, 120, 5148.
- 24  
25  
26 (8) Shin, J.-W.; Hammer, N. I.; Johnson, M. A.; Schneider, H.; Glöß, A.; Weber, J. M. *J. Phys. Chem.*  
27  
28  
29  
30  
31 A **2005**, 109, 3146.
- 32  
33  
34 (9) Nagata, T.; Yoshida, H.; Kondow, T. *Chem. Phys. Lett.* **1992**, 199, 205.
- 35  
36  
37 (10) Tsukuda, T.; Saeki, M.; Kimura, R.; Nagata, T. *J. Chem. Phys.* **1999**, 110, 7846.
- 38  
39  
40 (11) Saeki, M.; Tsukuda, T.; Iwata, S.; Nagata, T. *J. Chem. Phys.* **1999**, 111, 6333.
- 41  
42  
43 (12) Surber, E.; Mabbs, R.; Habteyes, T.; Sanov, A. *J. Phys. Chem. A* **2005**, 109, 4452.
- 44  
45  
46 (13) Muraoka, A.; Inokuchi, Y.; Nishi, N.; Nagata, T. *J. Chem. Phys.* **2005**, 122, 094303.
- 47  
48  
49 (14) Johnson, M. A.; Lineberger, W. C. In *Techniques in Chemistry*, Vol. 20; Farrar, J. M., Saunders,  
50  
51  
52  
53  
54 W. H., Eds.; Wiley, New York, 1988; p. 591.
- 55  
56 (15) Gaussian 98, Revision A.11.4, M. J. Frisch, G. W. Trucks, H. B. Schlegel, G. E. Scuseria, M. A.  
57  
58  
59  
60 Robb, J. R. Cheeseman, V. G. Zakrzewski, J. A. Montgomery, Jr., R. E. Stratmann, J. C. Burant,



1 S. Dapprich, J. M. Millam, A. D. Daniels, K. N. Kudin, M. C. Strain, O. Farkas, J. Tomasi, V.  
2 Barone, M. Cossi, R. Cammi, B. Mennucci, C. Pomelli, C. Adamo, S. Clifford, J. Ochterski, G. A.  
3 Petersson, P. Y. Ayala, Q. Cui, K. Morokuma, N. Rega, P. Salvador, J. J. Dannenberg, D. K.  
4 Malick, A. D. Rabuck, K. Raghavachari, J. B. Foresman, J. Cioslowski, J. V. Ortiz, A. G. Baboul,  
5 B. B. Stefanov, G. Liu, A. Liashenko, P. Piskorz, I. Komaromi, R. Gomperts, R. L. Martin, D. J.  
6 Fox, T. Keith, M. A. Al-Laham, C. Y. Peng, A. Nanayakkara, M. Challacombe, P. M. W. Gill, B.  
7 Johnson, W. Chen, M. W. Wong, J. L. Andres, C. Gonzalez, M. Head-Gordon, E. S. Replogle,  
8 and J. A. Pople (Gaussian, Inc., Pittsburgh PA, 2002).

9  
10  
11  
12  
13  
14  
15  
16  
17  
18  
19  
20 (16) Robertson, W. H.; Weddle, G. H.; Kelley, J. A.; Johnson, M. A. *J. Phys. Chem. A* **2002**, 106, 1205.

21  
22  
23 (17) Muraoka, A. Ph. D. Dissertation, The University of Tokyo, 2005.

24  
25  
26 (18) Robertson, W. H.; Price, E. A.; Weber, J. M.; Shin, J.-W.; Weddle, G. H.; Johnson, M. A. *J. Phys.*  
27  
28  
29  
30  
31  
32  
33  
34  
35  
36  
37  
38  
39  
40  
41  
42  
43  
44  
45  
46  
47  
48  
49  
50  
51  
52  
53  
54  
55  
56  
57  
58  
59  
60  
*Chem. A* **2003**, 107, 6527.

(19) Muraoka, A.; Inokuchi, Y.; Nagata, T. *J. Phys. Chem. A* **2008**, 112, 4906.

## Figure Captions

**Fig. 1.** Photoelectron spectra of  $(\text{CO}_2)_n^-$  (left panel) and  $[(\text{CO}_2)_n(\text{H}_2\text{O})]^-$  (right panel) with  $2 \leq n \leq 6$ . The spectra are reproduced from Ref. 10. The dots represent the experimental data while the solid curves are the best-fit Gaussian profiles. The shaded areas correspond to the band components associated with type II structures. Note that  $n$  represents the number of  $\text{CO}_2$  molecules in the cluster anions; the total number of constituents is  $n + 1$  for  $[(\text{CO}_2)_n(\text{H}_2\text{O})]^-$ .

**Fig. 2.** Overview of the infrared photodissociation spectra of  $[(\text{CO}_2)_n(\text{H}_2\text{O})]^-$  with  $n = 2 - 10, 14$  measured in the  $2800 - 3800 \text{ cm}^{-1}$ .

**Fig. 3.** Geometries of  $[(\text{CO}_2)_{2,3}(\text{H}_2\text{O})]^-$  optimized at the MP2/6-311++G\*\* level (Taken from Refs. 11 and 13). In referring to each isomeric form, the first digit of the notation “ $n\text{-}m\text{X}$ ” represents the number  $n$  of  $\text{CO}_2$  molecules involved in the cluster anion, the second digit the number  $m$  of  $\text{H}_2\text{O}$  molecules, and the last character “ $\text{X}$ ” is for identifying the individual structure. Bond lengths and angles are given in units of Angstroms and degrees. Net Mulliken charge populations for the constituent molecules are included in parentheses for each isomeric form.

**Fig. 4.** IPD spectra of  $[(\text{CO}_2)_4(\text{H}_2\text{O})]^-$  (top panel) compared with the stick diagrams of the calculated harmonic vibrational frequencies for the  $[(\text{CO}_2)_4(\text{H}_2\text{O})]^-$  isomeric forms optimized at the MP2/6-31+G\* level. One unit in the ordinate corresponds to the IR intensity of  $1000 \text{ km}\cdot\text{mol}^{-1}$ . Also shown on the right side are the corresponding optimized structures of the  $[(\text{CO}_2)_4(\text{H}_2\text{O})]^-$  isomers. Isomers **4-1A** – **4-1F** are the most stable representatives among those having the same hydrogen-bonding motifs.

**Fig. 5.** IPD spectra of the isotopically-substituted cluster anions with  $n = 4$  (upper panel): (a)  $[(\text{CO}_2)_4(\text{H}_2\text{O})]^-$ , (b)  $[(\text{CO}_2)_4(\text{HDO})]^-$  and (c)  $[(\text{CO}_2)_4(\text{D}_2\text{O})]^-$ . The spectral regions for the hydrogen-bonded OH stretching vibrations are highlighted in thick lines. In the lower panel, also shown for comparison are the calculated frequencies of the OH vibrations in (d)  $(\text{CO}_2)_3\cdot\text{CO}_2^- \cdots \text{H}-\text{OH}$ , (e)  $(\text{CO}_2)_3\cdot\text{CO}_2^- \cdots \text{H}-\text{OD}$  and (f)  $(\text{CO}_2)_3\cdot\text{CO}_2^- \cdots \text{D}-\text{OH}$  taking on the global minimum configuration **4-1D**.

1 One unit in the ordinate corresponds to the IR intensity of  $500 \text{ km}\cdot\text{mol}^{-1}$ . The frequency calculations are  
2 performed at the MP2/6-31+G\* level. Scaling factors for the calculated vibrational frequencies lie in  
3 the range 0.9486 – 0.9872, depending on the vibrational modes and isotopomers. These factors are  
4 determined so as to reproduce the normal-mode frequencies of an isolated H<sub>2</sub>O isotopomer. The tallest  
5 stick in each calculated spectrum corresponds to the hydrogen-bonded OH (OD) stretching vibration.  
6 The sticks marked with asterisks correspond to the free OH (OD) vibrations. The narrow sticks in gray  
7 indicate the frequency positions for the (harmonic)  $2\nu_2$  bending overtone along with the calculated  $\nu_2$   
8 frequencies in parentheses.  
9  
10  
11  
12  
13  
14  
15  
16  
17  
18  
19  
20  
21  
22  
23  
24  
25  
26  
27  
28  
29  
30  
31  
32  
33  
34  
35  
36  
37  
38  
39  
40  
41  
42  
43  
44  
45  
46  
47  
48  
49  
50  
51  
52  
53  
54  
55  
56  
57  
58  
59  
60

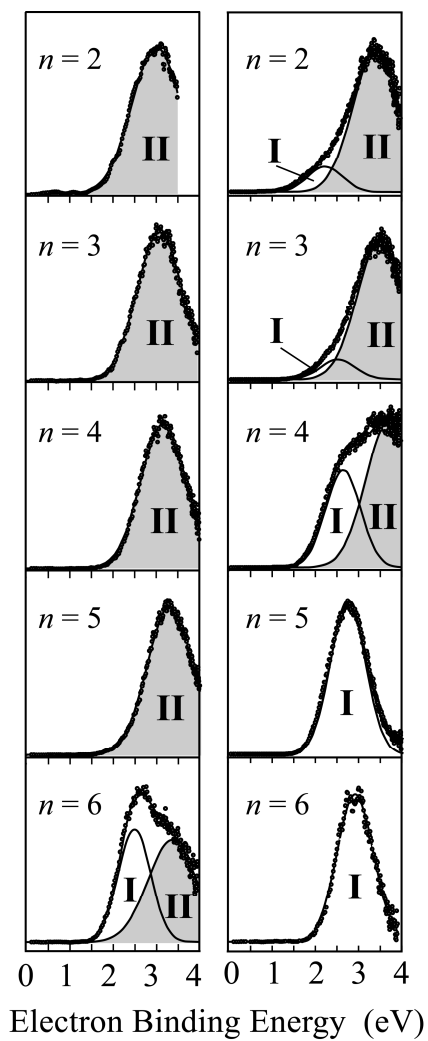


Figure 1. Muraoka *et al.*

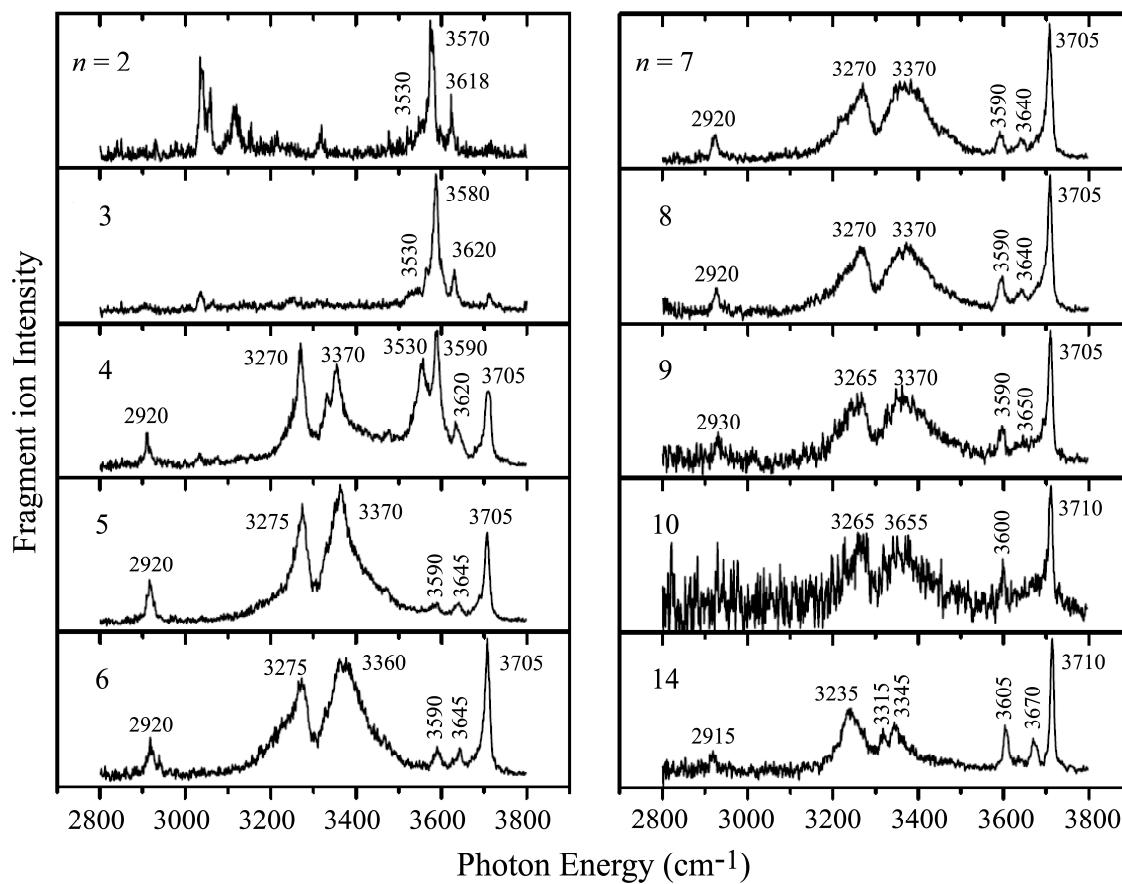


Figure 2. Muraoka *et al.*

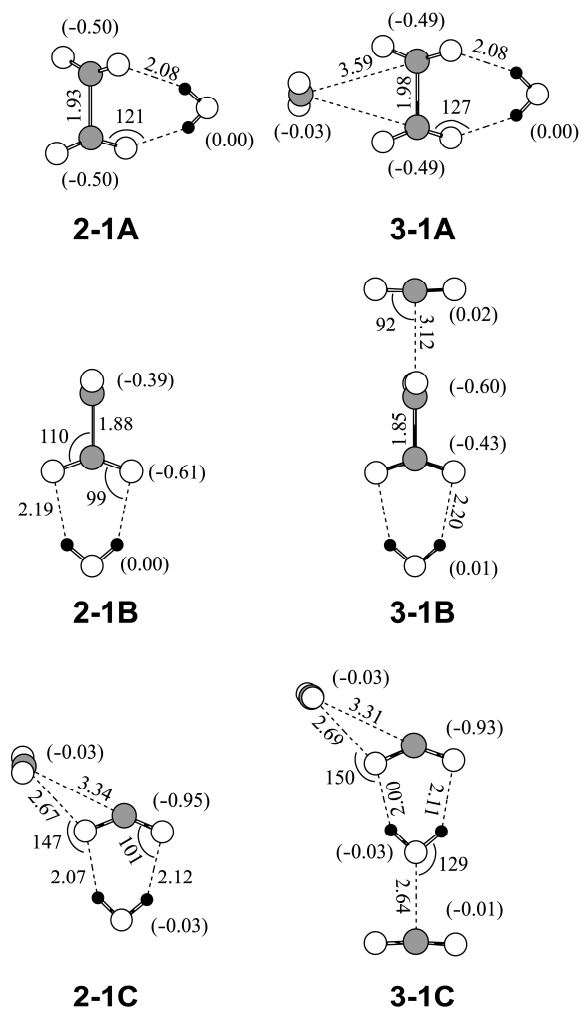


Figure 3. Muraoka *et al.*

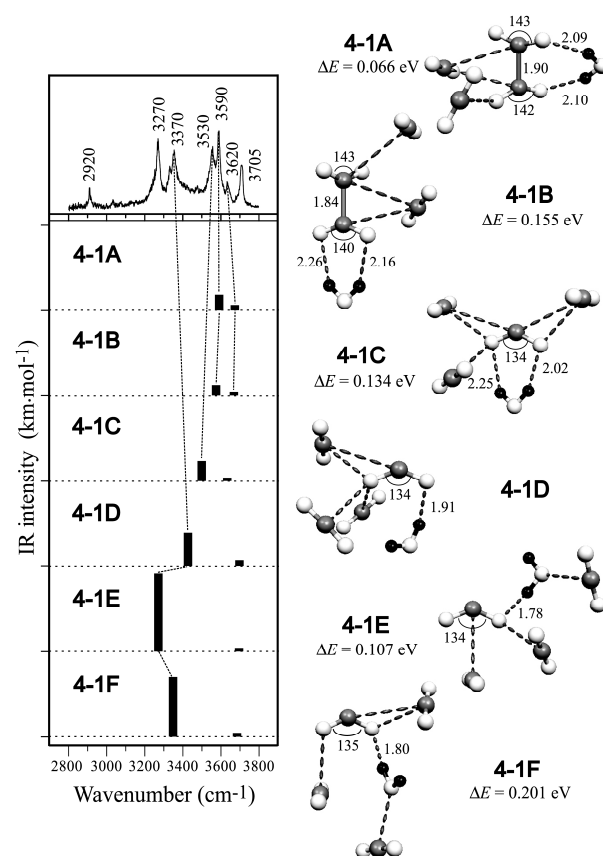


Figure 4. Muraoka *et al.*

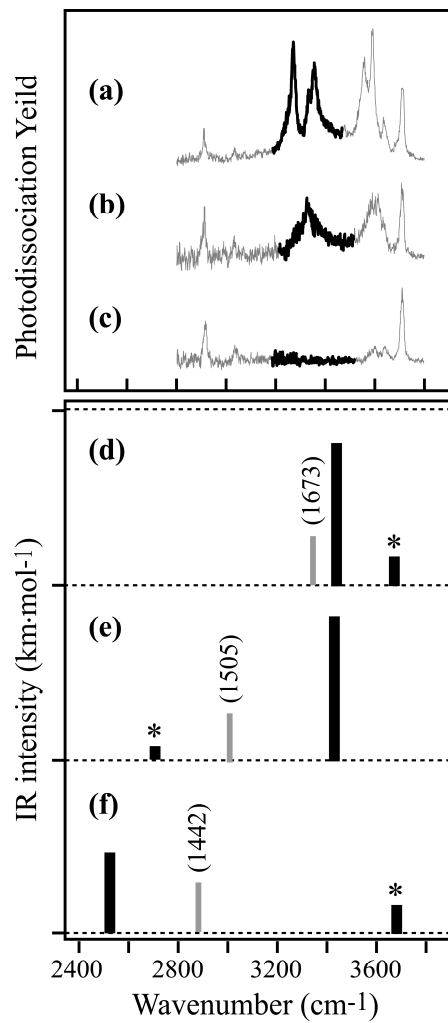


Figure 5. Muraoka *et al.*